

1 **Effect of renal ischaemia/reperfusion-induced acute kidney injury on**
2 **pharmacokinetics of midazolam in rats**

3

4 Ayako Tokunaga ¹, Hirotaka Miyamoto ¹, Shintaro Fumoto ¹ and Koyo Nishida ^{1,*}

5

6 1. Department of Pharmaceutics, Graduate School of Biomedical Science, Nagasaki

7 University, 1-7-1 Sakamoto, Nagasaki 852-8501, Japan

8 Tel.: +81-95-819-8567

9 Fax: +81-95-819-8567

10 E-mail: dds.yakuzai@gmail.com

11

12 ***Corresponding author**

13 Department of Pharmaceutics, Graduate School of Biomedical Science, Nagasaki

14 University, 1-7-1 Sakamoto, Nagasaki 852-8501, Japan

15 Tel.: +81-95-819-8567

16 Fax: +81-95-819-8567

17 E-mail: dds.yakuzai@gmail.com

18

19 **Abstract**

20 **Objectives**

21 This study aimed to investigate the effects of renal ischaemia/reperfusion (I/R)-
22 induced acute kidney injury (AKI) on the distribution of midazolam (MDZ), a probe
23 drug for cytochrome P450 3A (CYP3A) activities.

24 **Methods**

25 We established an AKI model inducing ischaemia of both renal pedicles for 60 min
26 followed by 24 h reperfusion. MDZ was administered intravenously (i.v.) to the rats via
27 the jugular vein and then blood samples were collected to determine the plasma
28 concentration of MDZ.

29 **Key findings**

30 While the plasma concentration of MDZ after i.v. administration was decreased in the
31 I/R rats, the tissue concentration was not altered. In addition, the tissue-to-plasma (T/P)
32 ratio of MDZ was increased in the I/R rats. The unbound fraction of MDZ and the level
33 of indoxyl sulphate (IS) in plasma was elevated in the I/R rats. Furthermore, the
34 unbound fraction of MDZ was significantly increased by the addition of IS.

35 **Conclusions**

36 These results indicated that the displacement of albumin-bound MDZ by IS changed

37 the unbound fraction of MDZ and elevated the T/P ratio of MDZ in I/R rats.

38

39 **Keywords:** Acute kidney injury, midazolam, protein binding, indoxyl sulphate,

40 distribution.

41

42 **Introduction**

43 Acute kidney injury (AKI) is a common complication occurring among hospitalised
44 patients. The incidence of AKI is increasing [1], and some studies have reported the
45 incidence as more than 20% among inpatients [2,3]. In some cases, AKI is induced by
46 drugs such as aminoglycosides, non-steroidal anti-inflammatory drugs, methotrexate,
47 cisplatin, and cyclosporine [4].

48 The renal clearance of drugs and toxins is altered in patients with AKI because it
49 affects glomerular filtration, tubular secretion, and renal drug metabolism [5].
50 Furthermore, AKI can affect the non-renal clearance of drugs and toxins by affecting
51 hepatic clearance [6]. The pharmacokinetics (PK) of drugs is determined not only by
52 metabolism but also by various other phenomena such as absorption and distribution.

53 Medication strategy in AKI patients is usually based on experimental rules or
54 extrapolated from that used in patients with chronic kidney disease (CKD) [7]. Several
55 studies have shown that CKD may alter the activities of transporters and cytochrome
56 P450 (CYP) [8]. Apart from evaluating the efficacy of drugs, the evaluation of PK in
57 renal disease is limited to assessment of the plasma concentration of drugs.
58 Furthermore, it is difficult to identify the factors affecting drug disposition because
59 various disorders are involved in AKI, which also varies in magnitude.

60 For optimising medications in AKI patients, factors affecting the PK of drugs should
61 be elucidated. Recently, various enzyme-specific probe drugs have been used for the
62 determination of enzyme activity *in vivo* [9]. Midazolam (MDZ) is often used as a probe
63 drug for CYP3A activities [10]. CYP3A is the most abundant phase I enzyme present in
64 the liver and intestine that metabolises approximately 50% of marketed drugs [11].
65 Therefore, in this study, we evaluated the PK of MDZ and assessed the factors affecting
66 its disposition in renal ischaemia/reperfusion (I/R)-induced AKI in a rat model.

67

68 **Materials and methods**

69 **Chemicals**

70 MDZ (Dormicum[®]) was purchased from Astellas Pharma Inc. (Tokyo, Japan).
71 Diazepam, Transaminase CII-test Wako, LabAssay[™] Creatinine, Evans Blue (EB), and
72 methyl *p*-hydroxybenzoate were from Wako Pure Chemical Industries Ltd. (Osaka,
73 Japan). Bromocresol green was obtained from Nacalai Tesque Inc. (Kyoto, Japan).
74 Bovine serum albumin (BSA) and indoxyl sulphate (IS) potassium salt were purchased
75 from Sigma-Aldrich (St. Louis, MO, USA). All other chemicals were of the highest
76 available purity.

77 **Animals**

78 Male Wistar rats (8-week-old) were obtained from CLEA Japan, Inc. (Tokyo, Japan)
79 and maintained on a standard laboratory diet (MF; Oriental Yeast, Co., Ltd, Tokyo,
80 Japan) and water *ad libitum*. All animal experiments conformed to the Guidelines for
81 Animal Experimentation of Nagasaki University (Nagasaki, Japan) and were approved
82 by the Committee on Animal Experimentation of Nagasaki University (approval no.
83 1607081322-2).

84 The abdominal cavity was incised, opened under sodium pentobarbital (50 mg/kg)
85 anaesthesia, and renal I/R was induced by placing vascular clamps over both renal
86 pedicles for 60 min followed by 24 h reperfusion. After the clamps were released, the
87 abdomens were closed using 4-0 sutures. Sham-operated rats underwent identical
88 surgical procedures, but both renal pedicles were not clamped. All animals received
89 saline (3 mL) instilled into the abdominal cavity during the surgical procedure. Serum
90 creatinine concentration, aspartate aminotransferase (AST), and alanine
91 aminotransferase (ALT) activities were estimated using the LabAssayTM creatinine or
92 transaminase CII-test Wako, respectively.

93 **Evaluation of MDZ PK**

94 The rats were anaesthetised with sodium pentobarbital (50 mg/kg, intraperitoneally
95 [i.p.]) and placed under a heat lamp to maintain the body temperature at 37°C. The

96 femoral artery was cannulated using a polyethylene tube (i.d. 0.5 mm, o.d. 0.8 mm,
97 Natsume Seisakusho, Co., Ltd., Tokyo, Japan).

98 MDZ (5 mg/kg) was administrated intravenously (i.v.) to the rats via the jugular vein
99 with anaesthesia maintained by pentobarbital. To determine the MDZ plasma
100 concentration, blood samples were collected 2, 5, 10, 20, 30, 45, and 60 min after
101 heparinised cannulas were inserted into the femoral arteries. The plasma samples were
102 obtained by centrifugation ($17,860 \times g$) at 25°C . To evaluate the tissue concentration of
103 MDZ, brain, liver, kidney, lung, and heart tissue samples were excised after 30 min,
104 weighed, and homogenised in 2-fold volumes of their weight in cold phosphate buffer at
105 pH 7.4.

106 The MDZ concentration was determined using high-performance liquid
107 chromatography (HPLC) including an ultraviolet detector following an established
108 method [12]. The plasma sample or tissue homogenate was mixed with 0.1 M NaOH
109 and 10 $\mu\text{g}/\text{mL}$ diazepam (internal standard) and then extracted using diethyl ether,
110 which was evaporated under nitrogen gas at 49°C and the dried sample was dissolved
111 in the mobile phase [acetate buffer, pH 4.7: acetonitrile 55:45 (v/v)].

112 The HPLC conditions were as follows: column, 5C₁₈-MS-II (Nacalai Tesque Inc.,
113 Kyoto, Japan); column temperature, 25°C ; mobile phase, acetate buffer, pH 4.7:

114 acetonitrile 55:45 (v/v); flow rate, 1 mL/min; and detector, SPD-20Av, 220 nm
115 (Shimadzu, Kyoto, Japan). For 100 μ L samples, the limit of quantitation (LOQ) of MDZ
116 was 62.5 ng/mL. The intra and inter-assay precision defined by the percentage of
117 relative standard deviation (RSD) were less than 10% across four concentration (312.5-
118 2500 ng/mL). The sample size for intra and inter-assay precision was three and eight,
119 respectively. The accuracies ranged from 83% to 105% across three concentration
120 (312.5-2500 ng/mL) in plasma, and other tissue homogenates showed similar trends.

121 **PK analysis**

122 The area under the plasma concentration-time curve (AUC_p) and mean residence time
123 (MRT_p) were analyzed by the non-compartment model. This analysis was performed by
124 numerical integration using a linear trapezoidal formula and extrapolating the data to
125 infinity time based on a mono-exponential equation. The total body clearance (CL_{tot})
126 and volume of distribution at steady state (V_{ss}) were calculated by dose/ AUC_p and
127 $CL_{tot} \cdot MRT_p$, respectively.

128 **Preparation of rat hepatocytes and incubation of drugs with hepatocytes**

129 Isolated rat hepatocytes were prepared from the livers of sham or I/R rats by
130 collagenase perfusion using an established method [12].

131 To investigate the effects of I/R on CYP3A activity, MDZ (0.25, 0.5, 1, 1.5, 2.5, 5, 7.5,

132 10 µg/mL) was incubated with rat hepatocytes diluted with Krebs-Henseleit buffer (1.0 ×
133 10⁶ cells/mL) at 37°C for 10 min. MDZ concentration linearly decreased for 10 min in
134 the rat hepatocytes (data not shown). After the incubation, the sample was mixed with
135 acetonitrile, centrifuged at 17,860 × g for 5 min, and the concentration of MDZ in the
136 supernatants was determined. The elimination velocity of MDZ from the incubation
137 sample was calculated using the following equation.

138
$$v = \frac{(C_0 - C_{10}) \times V}{10}$$

139 where the C₀ and C₁₀ are the concentrations of MDZ at 0 min and 10 min, respectively,
140 and V is the volume of incubation sample.

141 The Michaelis constant (K_m) and maximum elimination velocity (V_{max}) were obtained
142 by plotting the reciprocal of the velocity versus the reciprocal of the concentration
143 (Lineweaver-Burk plot). Apparent K_m and V_{max} values were calculated based on the
144 intercept on the X-axis and Y-axis of the Lineweaver-Burk plot, respectively,

145
$$\frac{1}{v} = \frac{K_m + C}{V_{max} \cdot C}$$

146 where v is the elimination velocity, C is the concentration of MDZ, K_m is the Michaelis
147 constant, and V_{max} is the maximum elimination velocity. Hepatic intrinsic clearance
148 (CL_{int}) was calculated by V_{max}/K_m.

149 **Plasma volume determination**

150 The plasma volumes were estimated using the EB dye technique. EB binds almost
151 exclusively to plasma albumin and is used to determine plasma volume [13,14]. EB-
152 BSA was prepared using the following method: EB and BSA were dissolved in saline,
153 and the resultant EB-BSA (40 mg/mL) was purified using gel filtration.

154 A baseline blood sample (400 μ L) was collected by inserting a heparinised cannula
155 into the femoral artery prior to plasma volume determination and a comparable volume
156 of sterile saline was infused. Then, a bolus dose of EB-BSA solution (1 mL/kg) was
157 injected into the femoral artery. After 5 min, a second blood sample (400 μ L) was
158 withdrawn. The plasma was diluted 20-fold with saline, and the absorbance was
159 determined at 605 nm (UV-1600, Shimadzu, Kyoto, Japan). The plasma volume was
160 calculated using the following equation:

$$161 \quad \text{Plasma volume (mL/kg)} = \frac{\text{Injected EB-BSA } (\mu\text{g}) / \text{EB in plasma } (\mu\text{g/mL})}{\text{body weight (kg)}}$$

162 **Evaluation of serum albumin concentration**

163 According to a previously described procedure [15], 1.0 mL bromocresol green (50
164 μ M) in citrate buffer (pH 4.0) was added to 10 μ L serum and kept at room temperature
165 for 10 min. The absorbance of these solutions was determined (UV-1600) at 628 nm.
166 The standard curves were prepared with BSA in saline.

167 **Determination of MDZ unbound fraction in plasma**

168 The unbound fraction of MDZ in the plasma was determined using the erythrocyte
169 versus buffer or plasma partitioning method [16,17]. Briefly, sham and I/R rats were
170 anaesthetised with sodium pentobarbital (50 mg/kg, i.p.), blood samples were collected
171 from the inferior vena cava, and centrifuged ($2,500 \times g$) at room temperature for 10
172 min. After removing the plasma and buffy-coat layers, the blood cells were gently
173 washed three times in 500 μ L phosphate-buffered saline (PBS, pH 7.4). Then, either
174 PBS or plasma (diluted 10-fold with PBS) was added to yield a haematocrit (HCT) of
175 0.3. The MDZ solution was then added to each suspension to final concentrations of 500
176 or 5000 ng/mL. The mixtures were incubated in a water bath for 1 h at 37°C. After
177 centrifugation at $9,000 \times g$ for 10 min, the MDZ concentration in the supernatant was
178 determined using HPLC, as described above.

179 The unbound fraction (f_u) was calculate as described below [16,17]. The erythrocyte
180 concentration of MDZ in the plasma diluted 10 times with PBS (C_E) was determined
181 using the following equation:

$$182 \quad C_E = \frac{C_B - C_P \times (1 - \text{HCT})}{\text{HCT}}$$

183 where C_B and C_P are the total concentration of MDZ in the blood suspension and
184 supernatant, respectively.

185 Likewise, to estimate the erythrocyte concentration of MDZ in PBS (C_E^*), the total

186 MDZ concentrations in the suspension (C_B^*) and supernatant (C_P^*) were substituted for

187 C_P and C_B , respectively. The f_u values were determined as:

$$188 \quad f_u' = \frac{P_{E/P}}{P_{E^*/P^*}}$$

$$189 \quad f_u = 100 \times \frac{d \times f_u'}{1 - f_u' \times (1 - d)}$$

190 where f_u is the unbound fraction in the diluted plasma and d is the dilution factor (e.g., d

191 = 0.1 for a 10-fold plasma dilution). The partition coefficients of erythrocytes to diluted

192 plasma or PBS are represented by $P_{E/P}$ (C_E/C_P) and P_{E^*/P^*} (C_E^*/C_P^*), respectively.

193 **Determination of IS in plasma**

194 The IS concentration was estimated using HPLC fluorescence detection [18]. The

195 plasma samples were stored at -80°C and thawed at room temperature before

196 processing. Plasma samples were mixed with 1 mg/mL methyl *p*-hydroxybenzoate

197 dissolved in methanol (internal standard), kept at room temperature for 10 min,

198 centrifuged ($17,860 \times g$) at 25°C for 5 min, and the supernatants were injected into the

199 chromatographic system.

200 The HPLC conditions were as follows: column, InertSustain[®] C18 (GL Sciences Inc.,

201 Tokyo, Japan); column temperature, 40°C ; mobile phase, acetate buffer, pH 4.7:

202 acetonitrile 80:20 (v/v); flow rate, 1.3 mL/min; detector, RF-20A (Shimadzu, Kyoto,

203 Japan). The excitation and emission wavelengths were 280 and 375 nm, respectively.

204 For 20 μL samples, the intra and inter-assay precision defined by the percentage of RSD
205 was less than 10% across four concentration (3.125-25 μM). The sample size for intra
206 and inter-assay precision was three and eight, respectively. The accuracies ranged from
207 93% to 106% across three concentration (3.125-25 μM) in plasma.

208 **Effects of IS on MDZ protein binding**

209 To further investigate possible competitive interactions with IS in I/R rats, the
210 unbound fraction of MDZ to IS was determined using the erythrocyte versus buffer or
211 plasma partitioning method after adding IS at a physiologically achievable
212 concentration. Briefly, untreated rats were anaesthetised with sodium pentobarbital (50
213 mg/kg, i.p.), and blood samples were collected from the inferior vena cava. Blood cells
214 were collected as described in the method of “Determination of MDZ unbound fraction
215 in plasma”. Blood samples were centrifuged ($2,500 \times g$) at room temperature for 10
216 min, the plasma and buffy-coat layers were removed, and blood cells were gently
217 washed three times in 500 μL PBS. PBS or plasma (diluted 10-times with PBS or PBS
218 plus IS [500 μM]) was added to the blood cells to yield an HCT of 0.3. The MDZ
219 solution was then added to each suspension to final concentrations of 5000 ng/mL. The
220 f_u of MDZ in each sample was determined as described in the method of “Determination
221 of MDZ unbound fraction in plasma”.

222 **Statistical analyses**

223 We performed Student's *t*-test using JMP 14 (SAS Institute Inc., Cary, NC, USA) and
224 $p < 0.05$ was considered statistically significant.

225

226 **Results**

227 **Biochemical assays**

228 Serum creatinine concentration was used to assess the degree of AKI induced by
229 renal I/R. As shown in Table 1, 24 h after surgery, the serum creatinine concentration
230 was significantly increased in the I/R rats compared to that in the sham rats. Moreover,
231 renal I/R led to a rise in serum AST and ALT activities relative to the sham rats.

232 **Effects of renal I/R on MDZ PK**

233 Figure 1 shows the plasma concentration-time curves of MDZ after i.v.
234 administration to sham or I/R rats. The plasma concentration of MDZ in the I/R rats was
235 markedly lower than that of the sham rats. The AUC_p , MRT_p , CL_{tot} , and V_{ss} of MDZ are
236 listed in Table 2. The AUC_p of I/R rats was decreased by approximately 40% compared
237 to that of the sham rats. On the other hand, the MRT_p was not altered between the sham
238 and I/R rats. The CL_{tot} and V_{ss} of MDZ were significantly increased in the I/R rats
239 compared to the sham rats.

240 [Insert Figure 1 here]

241

242 **Effects of I/R on MDZ metabolism in rat hepatocytes**

243 Figure 2 shows the Lineweaver-Burk plot for MDZ elimination from rat hepatocytes.

244 No significant changes were observed in the CL_{int} of MDZ between the sham ($0.18 \pm$

245 0.0049 , $n=5$) and I/R (0.17 ± 0.0074 , $n=4$) rats.

246 [Insert Figure 2 here]

247

248 **Effects of renal I/R on MDZ tissue distribution**

249 The tissue concentrations of MDZ 30 min after i.v. administration to the rats are

250 shown in Figure 3. The MDZ concentration in the analysed tissues was not affected by

251 renal I/R. Figure 4 shows the tissue-to-plasma (T/P) ratios of MDZ 30 min after i.v.

252 administration, which was significantly increased in the I/R rats.

253 [Insert Figures 3 and 4 here]

254

255 **Plasma volume determination and evaluation of serum albumin concentration**

256 We estimated the plasma volume and serum albumin concentration of sham and I/R

257 rats to investigate the effects of I/R on V_{ss} . The plasma volume was not significantly

258 different between the sham and I/R rats (38.6 ± 0.73 [n=3] and 43.4 ± 2.00 [n=5]
259 mL/kg, respectively). In addition, the serum albumin concentrations did not change
260 between sham and I/R rats (3.34 ± 0.80 [n=3] and 4.35 ± 0.22 [n=3] g/dL,
261 respectively).

262 **Alteration of unbound MDZ fraction in I/R rats**

263 The plasma unbound fraction of MDZ in the sham and I/R rats at a concentration of
264 500 or 5000 ng/mL is shown in Table 3. The MDZ concentration range corresponded
265 to the MDZ plasma concentration profiles in the PK study. The plasma unbound
266 fractions of each I/R rat samples were significantly higher than those of the sham rats
267 were.

268 **Determination of IS concentration in plasma**

269 Various uremic toxins that are normally excreted in the urine are accumulated in the
270 circulatory system in renal dysfunction. Among these uremic toxins, IS is markedly
271 increased in the serum in renal disease and it binds strongly to albumin [19]. In the
272 present study, the plasma IS concentration was elevated by more than 10 times in the
273 I/R rats than that in the sham rats (Figure 5).

274 **[Insert Figure 5 here]**

275

276 **Effect of IS on protein binding of MDZ**

277 To further investigate whether IS participates in increasing the unbound fraction of
278 MDZ, we evaluated the unbound MDZ ratio in the presence of 500 μ M IS. This IS
279 concentration corresponded to the approximate value observed in the plasma in I/R rats.
280 The unbound fraction of MDZ was significantly increased in the presence of IS (Figure
281 6).

282 **[Insert Figure 6 here]**

283
284 **Discussion**

285 Several diseases such as CKD or AKI can change the disposition of various drugs
286 [20]. Many studies have evaluated the effects of CKD on the PK of drugs, focusing on
287 hepatic metabolism [21] because the liver is mainly responsible for drug metabolism. In
288 contrast, there are few reports on the alteration of drug distribution in kidney injury
289 despite the fact that the tissue concentrations of drugs have an impact on their effects.
290 Therefore, we aimed to elucidate the PK behaviour of MDZ, which undergoes hepatic
291 metabolism and evaluated its disposition in a rat model of AKI. Specifically, we focused
292 on the effect of AKI on MDZ distribution, protein binding, and tissue concentration.

293 In the present study, we used renal I/R rats as an experimental AKI model. A

294 significant increase in serum creatinine concentration (Table 1) was observed, indicating
295 that AKI was established by renal I/R. Furthermore, the marked increase in AST and
296 ALT activities (Table 1) suggested that hepatic dysfunction also occurred with AKI, and
297 the findings were similar to those of a previous study using an AKI rat model [22].

298 The plasma concentration of MDZ after i.v. administration was markedly decreased
299 in the I/R rats (Figure 1). Furthermore, the CL_{tot} and V_{ss} were increased in the I/R rats
300 (Table 2).

301 The metabolism of MDZ is mediated primarily by CYP3A and MDZ has intermediate
302 hepatic extraction [23]. Therefore, based on the well-stirred model of hepatic clearance,
303 MDZ clearance depends on hepatic blood flow, CL_{int} and unbound fraction. Indocyanine
304 green (ICG) clearance depends on hepatic blood flow and is used for quantifying
305 hepatic blood flow [24]. Although we evaluated the effect of ICG clearance on I/R-
306 induced AKI, ICG clearance remained unchanged in I/R rats (data not shown).

307 Moreover, to investigate the effects of I/R on CL_{int} , MDZ was incubated with rat
308 hepatocytes to calculate the CL_{int} by Lineweaver-Burk plot (Figure 2). No significant
309 changes were observed in the CL_{int} between the sham and I/R rats. Therefore, the
310 alteration in clearance of MDZ depends on the change in MDZ unbound fraction. In
311 particular, because MDZ is highly bound in plasma (approximately 95%), its

312 pharmacokinetics is susceptible to unbound fraction.

313 To evaluate the effects of I/R on MDZ distribution in tissues, the MDZ concentration
314 in the tissues was determined. While the plasma concentration of MDZ was decreased
315 in the I/R rats, the tissue concentration was not altered except in the kidneys (Figure 3).

316 The pathogenic mechanism underlying renal I/R injury involves tubular necrosis and
317 apoptosis, inflammation, and oxidative stress [25]. These damages provoke increasing
318 vascular permeability, interstitial edema, and compromise in renal blood flow [26].

319 Since the kidney is rich in blood flow, a decrease in renal blood flow might have led to a
320 decrease in renal concentration of MDZ. In addition, the T/P of MDZ was increased in
321 the I/R rats (Figure 4). The V_{ss} is captured in the equation

322
$$V_{ss} = V_{plasma} + V_{tissue} \times K_p$$

323 where the V_{plasma} and V_{tissue} are the volumes of plasma and tissue, and K_p is the T/P
324 concentration ratio which in turn is influenced by the unbound ratio of plasma and tissue,
325 respectively. Plasma volume was not changed between sham and I/R rats. Therefore, as
326 when K_p increases, V_{ss} is expected to increase.

327 Further, protein binding was evaluated to investigate the factors affecting the T/P
328 ratio of MDZ. In this study, we determined the unbound fraction of MDZ using the
329 erythrocyte versus buffer or plasma partitioning method. We found that the plasma

330 unbound fraction obtained by this method was approximately 5% in sham rats, which is
331 similar to that previously reported in humans using equilibrium dialysis [27,28]. The
332 unbound fraction of MDZ in the plasma was increased in the I/R rats compared to the
333 sham rats (Table 3). Serum albumin concentration did not alter between sham and I/R
334 rats. These results indicated that the unbound fraction of MDZ increased because of
335 protein displacement, and not a reduction of plasma albumin concentration.

336 Uremic syndrome is attributed to the cumulation of various compounds, which are
337 normally eliminated by healthy kidneys. These compounds are called uremic toxins
338 when they exert negative influences on the human body. Approximately 100 uremic
339 toxins have been reported [29]. Among these uremic toxins, protein-bound solutes such
340 as IS, 3-carboxy-4-methyl-5-propyl-2-furanpropanoic acid (CMPF), *p*-cresyl sulphate
341 (PCS), and indoleacetic acid (IA) bind strongly to plasma protein, mostly albumin. IS,
342 PCS, and IA mainly bind to site II of albumin where MDZ binds. On the other hand,
343 CMPF mainly binds to site I of albumin [30,31]. The plasma IS level was increased by
344 more than 10 times in the I/R rats (Figure 5) compared to levels in the sham rats. The
345 plasma concentrations of IA and PCS were also evaluated, but the increase was not as
346 great as that which was observed for IS (data not shown). Furthermore, the unbound
347 fraction of MDZ was significantly increased after the addition of IS (Figure 6), similarly

348 to that of I/R rats. Thus, the change in the unbound fraction of MDZ in plasma could be
349 explained by the displacement of albumin-bound MDZ by IS.

350 Our results showed that the plasma concentration of MDZ decreased in the I/R-
351 induced AKI, and resulted from displacement of binding between MDZ and albumin by
352 IS. However, Kirwan CJ *et al* reported that the plasma concentration of MDZ increased
353 in critically ill patients, and concluded that increasing severity and duration of AKI were
354 associated with decreased MDZ elimination[32]. These critically ill patients with AKI
355 had various complications including CKD, and took other medicines such as alfentanil,
356 which were also metabolized by CYP3A. Additionally, there was a lack of hepatic blood
357 flow and unbound fraction of MDZ in critically ill patients. Each of these aspects
358 complicates our understanding of PK in AKI. Further studies are needed in order to fill
359 in the gaps between human studies and animal studies.

360

361 **Conclusions**

362 In this study, we found that the plasma concentration of MDZ decreased in the I/R
363 rats, while the tissue concentration did not change. The accumulated IS in the I/R rats
364 inhibited the binding of MDZ to albumin, which increased the unbound fraction of
365 MDZ. These results could provide new insights into drug administration in AKI.

366

367 **Funding**

368 This work was supported by JSPS KAKENHI (grant no. 16K18947).

369

370 **References**

- 371 1. Rewa O, Bagshaw SM. Acute kidney injury-epidemiology, outcomes and
372 economics. *Nat Rev Nephrol* 2014; 10: 193-207.
- 373 2. Wang HE *et al.* Acute kidney injury and mortality in hospitalized patients. *Am J*
374 *Nephrol* 2012; 35: 349-355.
- 375 3. Koza Y. Acute kidney injury: current concepts and new insights. *J Inj Violence*
376 *Res* 2016; 8: 58-62.
- 377 4. Naughton CA. Drug-induced nephrotoxicity. *Am Fam Physician* 2008; 78: 743-
378 750.
- 379 5. Vilay AM *et al.* Clinical review: Drug metabolism and nonrenal clearance in
380 acute kidney injury. *Crit Care* 2008; 12: 235.
- 381 6. Matzke GR *et al.* Drug dosing consideration in patients with acute and chronic
382 kidney disease—a clinical update from Kidney Disease: Improving Global
383 Outcomes (KDIGO). *Kidney Int* 2011; 80: 1122-1137.

- 384 7. Dixon J *et al.* Xenobiotic metabolism: the effect of acute kidney injury on non-
385 renal drug clearance and hepatic drug metabolism. *Int J Mol Sci* 2014; 15: 2538-
386 2553.
- 387 8. Michaud J *et al.* Effects of serum from patients with chronic renal failure on rat
388 hepatic cytochrome P450. *Br J Pharmacol* 2005; 144: 1067-1077.
- 389 9. Kivisto KT, Kroemer HK. Use of probe drugs as predictors of drug metabolism
390 in humans. *J Clin Pharmacol* 1997; 37: 40S-48S.
- 391 10. Kirwan CJ *et al.* Using midazolam to monitor changes in hepatic drug
392 metabolism in critically ill patients. *Intensive Care Med* 2009; 35: 1271-1275.
- 393 11. Guengerich FP. Cytochrome P450s and other enzymes in drug metabolism and
394 toxicity. *AAPS J* 2006; 8: E101-111.
- 395 12. Miyamoto H *et al.* Evaluation of hypothermia on the in vitro metabolism and
396 binding and in vivo disposition of midazolam in rats. *Biopharm Drug Dispos*
397 2015; 36: 481-489.
- 398 13. Klemcke HG *et al.* Genetic influences on survival time after severe hemorrhage
399 in inbred rat strains. *Physiol Genomics* 2011; 43: 758-765.
- 400 14. Rose R, Klemcke HG. Relationship between Plasma Albumin Concentration and
401 Plasma Volume in 5 Inbred Rat Strains. *J Am Assoc Lab Anim Sci* 2015; 54: 459-

- 402 464.
- 403 15. Kishikawa N *et al.* A novel lophine-based fluorescence probe and its binding to
404 human serum albumin. *Anal Chim Acta* 2013; 780: 1-6.
- 405 16. Schuhmacher J *et al.* Determination of the free fraction and relative free fraction
406 of drugs strongly bound to plasma proteins. *J Pharm Sci* 2000; 89: 1008-1021.
- 407 17. Kobuchi S *et al.* Pharmacokinetics and distribution of fluvoxamine to the brain
408 in rats under oxidative stress. *Free Radic Res* 2012; 46: 831-841.
- 409 18. Al Za'abi M *et al.* HPLC-fluorescence method for measurement of the uremic
410 toxin indoxyl sulfate in plasma. *J Chromatogr Sci* 2013; 51: 40-43.
- 411 19. Watanabe H *et al.* Update on the pharmacokinetics and redox properties of
412 protein-bound uremic toxins. *J Pharm Sci* 2011; 100: 3682-3695.
- 413 20. Nolin TD *et al.* Hepatic drug metabolism and transport in patients with kidney
414 disease. *Am J Kidney Dis* 2003; 42: 906-925.
- 415 21. Dowling TC *et al.* Characterization of hepatic cytochrome P4503A activity in
416 patients with end-stage renal disease. *Clin Pharmacol Ther* 2003; 73: 427-434.
- 417 22. Golab F *et al.* Ischemic and non-ischemic acute kidney injury cause hepatic
418 damage. *Kidney Int* 2009; 75: 783-792.
- 419 23. Rogers JF *et al.* An evaluation of the suitability of intravenous midazolam as an

- 420 in vivo marker for hepatic cytochrome P4503A activity. *Clin Pharmacol Ther*
421 2003; 73: 153-158.
- 422 24. Ma JD *et al.* Quantitative assessment of hepatic blood flow using intravenous
423 indocyanine green. *Eur J Clin Pharmacol* 2008; 64: 1133-1134.
- 424 25. Eltzhig HK, Eckle T. Ischemia and reperfusion--from mechanism to
425 translation. *Nat Med* 2011; 17: 1391-1401.
- 426 26. Zuk A, Bonventre JV. Acute Kidney Injury. *Annu Rev Med* 2016; 67: 293-307.
- 427 27. Jones DR *et al.* Brain uptake of benzodiazepines: effects of lipophilicity and
428 plasma protein binding. *J Pharmacol Exp Ther* 1988; 245: 816-822.
- 429 28. Allonen H *et al.* Midazolam kinetics. *Clin Pharmacol Ther* 1981; 30: 653-661.
- 430 29. Vanholder R *et al.* Review on uremic toxins: classification, concentration, and
431 interindividual variability. *Kidney Int* 2003; 63: 1934-1943.
- 432 30. Sakai T *et al.* Characterization of binding site of uremic toxins on human serum
433 albumin. *Biol Pharm Bull* 1995; 18: 1755-1761.
- 434 31. Watanabe H *et al.* Interaction between two sulfate-conjugated uremic toxins, p-
435 cresyl sulfate and indoxyl sulfate, during binding with human serum albumin.
436 *Drug Metab Dispos* 2012; 40: 1423-1428.
- 437 32. Kirwan CJ *et al.* Acute kidney injury reduces the hepatic metabolism of

438 midazolam in critically ill patients. *Intensive Care Med* 2011; 38: 76-84.

439

440 **Tables**

441 **Table 1.** Biochemical parameters of serum from sham and ischaemia/reperfusion (I/R)

442 rats

	Sham	I/R
Creatinine (mg/dL)	0.63 ± 0.08	3.70** ± 0.52
AST (IU/L)	42.7 ± 2.7	163.5 ± 76.7
ALT (IU/L)	12.7 ± 1.0	22.0* ± 2.8

443 Each value represents mean ± standard error (S.E.) of three experiments (* $p < 0.05$ and

444 ** $p < 0.01$ vs. sham rats).

445

446 **Table 2.** Moment parameters after intravenous (i.v.) administration of midazolam (5
447 mg/kg) to sham and ischaemia/reperfusion (I/R) rats

	Sham	I/R
AUC_p (ng · min/mL)	67880 ± 4555	38891 ^{**} ± 3135
MRT_p (min)	36.3 ± 1.0	36.0 ± 0.9
CL_{tot} (mL/min)	18.7 ± 1.0	33.9 ^{**} ± 1.6
V_{ss} (mL)	679.5 ± 47.4	1217.4 ^{**} ± 32.7

448 Each value represents mean ± standard error (S.E.) of three (sham) or four (I/R)
449 experiments (^{**}*p* < 0.01 vs. sham rats).

450

451 **Table 3.** Plasma unbound fraction of midazolam in sham and ischaemia/reperfusion

452 (I/R) rats

MDZ concentration (ng/mL)	Sham	I/R
500	5.05 ± 0.43	8.20** ± 0.60
5000	5.19 ± 0.36	6.94** ± 0.31

453 Each value represents mean ± standard error (S.E.). n=5 for sham experiment, n=4 for

454 500 ng/mL of I/R and n=5 for 5000 ng/mL of I/R (***p* < 0.01 vs. sham rats).

455

456 **Figure legends**

457 **Figure 1.** Plasma concentration-time profiles of midazolam (5 mg/kg) after intravenous
458 (i.v.) administration to sham (○) and ischaemia/reperfusion (I/R) (■) rats. Each
459 symbol represents mean ± standard error (S.E.) of three (sham) or four (I/R)
460 experiments.

461 **Figure 2.** Lineweaver-Burk plot for the elimination rate of midazolam in rat hepatocytes
462 from sham (○) and ischaemia/reperfusion (I/R) (■) rats. Each symbol represents mean
463 ± standard error (S.E.) of five (sham) or four (I/R) experiments.

464 **Figure 3.** Midazolam (5 mg/kg) concentration in tissues after intravenous (i.v.)
465 administration to sham (□) and ischaemia/reperfusion (I/R) (■) rats. The tissue samples
466 were collected 30 min after administration. Each bar represents mean + standard error
467 (S.E.) of six (sham) or five (I/R) experiments ($^{**}p < 0.01$ vs. sham rats).

468 **Figure 4.** Tissue-to-plasma ratio (T/P) of midazolam (5 mg/kg) after intravenous (i.v.)
469 administration to sham (□) and ischaemia/perfusion (I/R) (■) rats. The plasma and tissue
470 samples were collected 30 min after administration. Each bar represents mean +
471 standard error (S.E.) of six (sham) or five (I/R) experiments ($^{*}p < 0.05$ and $^{**}p < 0.01$
472 vs. sham rats).

473 **Figure 5.** Plasma concentration of indoxyl sulphate (IS) in sham or
474 ischaemia/reperfusion (I/R) rats. Each bar represents mean + standard error (S.E.) of
475 eight (sham) or nine (I/R) experiments ($**p < 0.01$ vs. sham rats).

476 **Figure 6.** Effects of indoxyl sulphate (IS) on midazolam protein binding. Each bar
477 represents mean + standard error (S.E.) of four experiments ($**p < 0.01$ vs. normal).

Figure 1.

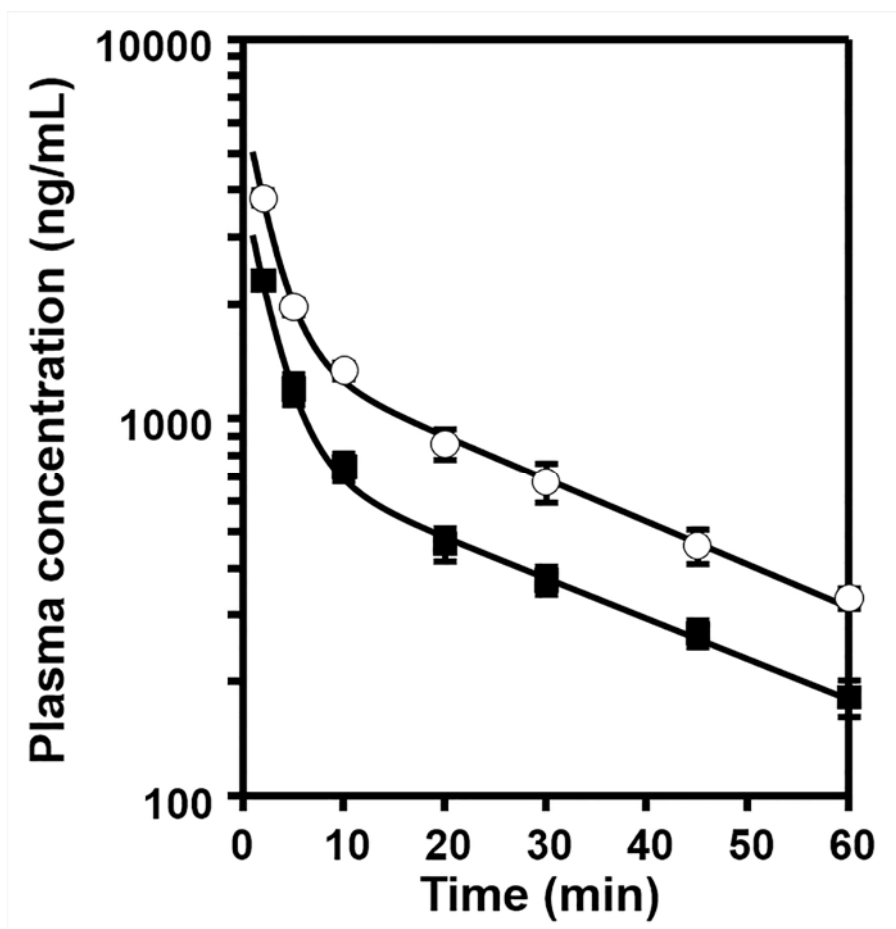


Figure 2.

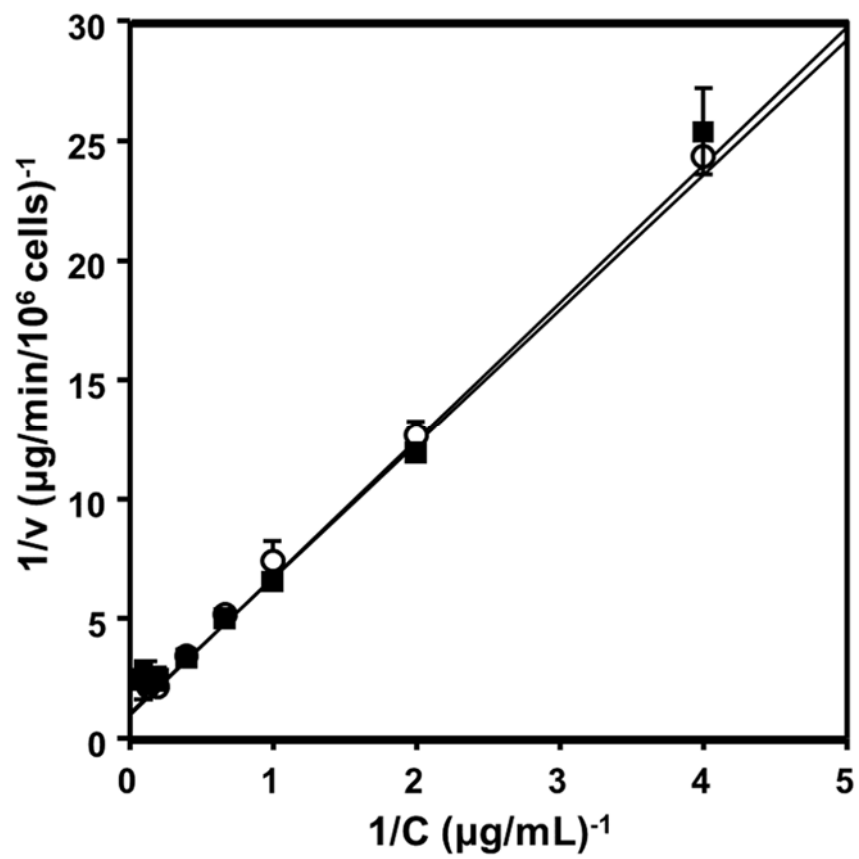


Figure 3.

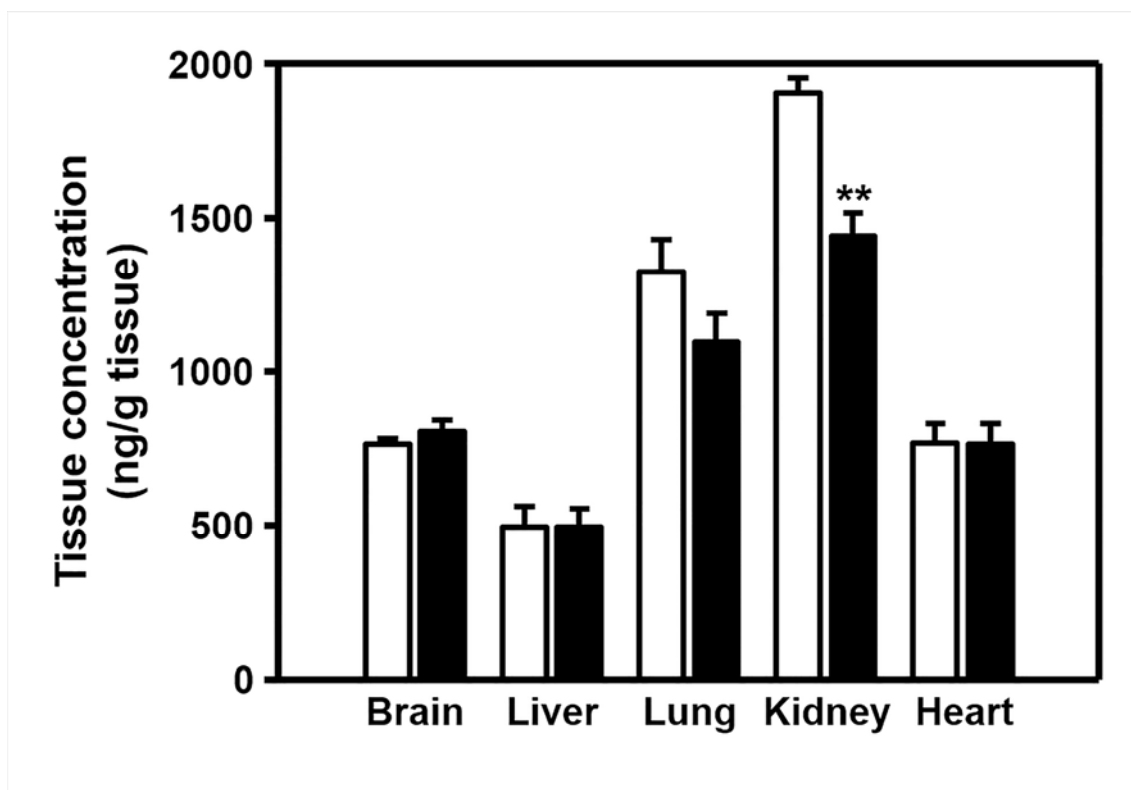


Figure 4.

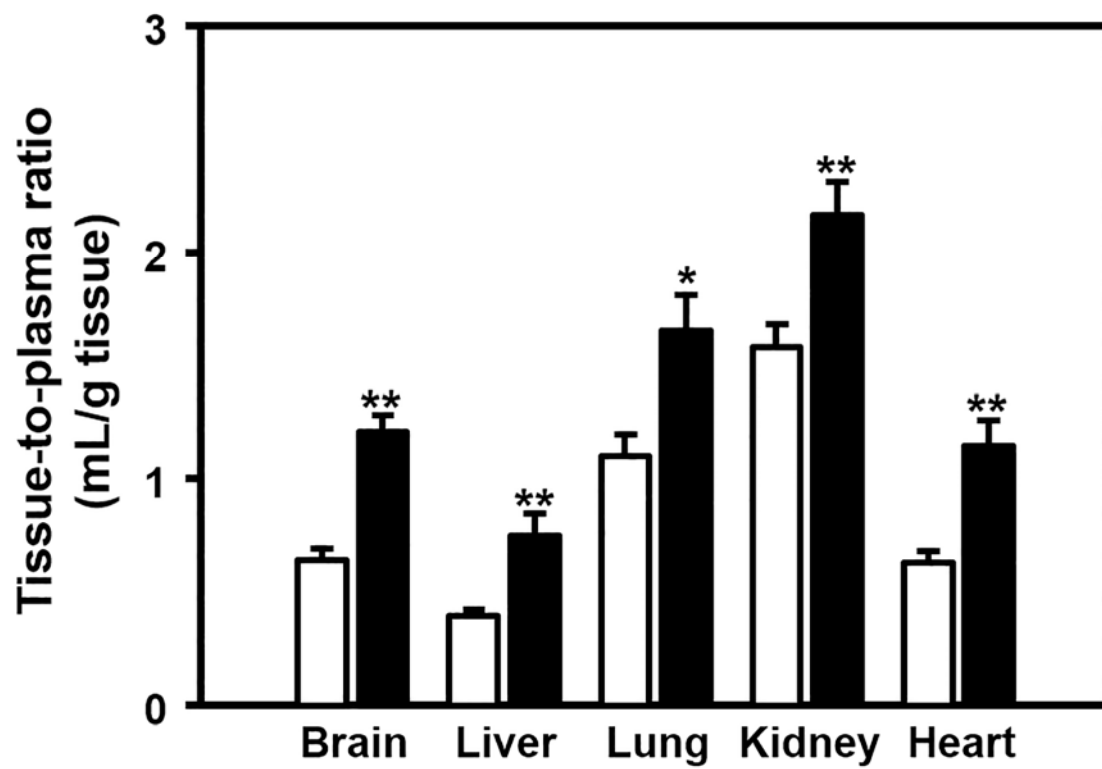


Figure 5.

